Proceedings of the 20th International Conference on Soil Mechanics and Geotechnical Engineering– Rahman and Jaksa (Eds)

Pile behavior in a long-term loaded piled raft foundation model on saturated clay

Comportement des pieux dans un modèle de fondation de radier chargé à long terme sur de l'argile saturée

Lua Hoang
Faculty of Civil Engineering, Thuyloi University, Vietnam, hoangthilua@tlu.edu.vn

Tatsunori Matsumoto
Graduate School of Natural Science and Technology, Kanazawa University, Japan

ABSTRACT: This paper aims to investigate the long-term behavior of a piled raft foundation (PRF) through small-scale physical modeling, in which the main focus was placed on the pile response. In the experiments, the model ground was prepared by consolidating a slurry clayey soil. The model foundation consisted of a square raft having a width of 125 mm, and 16 piles having a length of 150 mm and a diameter of 10 mm. For the loading test of the PRF, vertical load was increased by multiple steps and each load step was maintained to observe the long-term behavior. The experimental results showed that the level of applied load affects the load sharing between the raft and the piles, and also affects the load sharing between the piles. The piles were effective at supporting load and suppressing PRF settlement when the applied load was smaller than the ultimate capacity of the corresponding pile group. The shaft resistances of peripheral piles were mobilized from the low levels of the applied load meanwhile the loads on center piles were mainly supported by the pile tip sections at these load steps. The shaft resistances of center piles were mobilized at the higher levels of the applied load when the applied load exceeded the ultimate capacity of the pile group.

RÉSUMÉ: Ce document présente le comportement à long terme d'un radier de fondation sur pieux (RFP) en utilisant une modélisation physique à petite échelle, dans laquelle le principal objectif est la réaction des pieux. Le sol modèle a été préparé en consolidant un sol argileux boueux. La fondation modèle était constituée d'un radeau carré et de 16 pieux. Pour le test de charge du PRF, la charge verticale a été augmentée de plusieurs étapes et chaque étape de charge a été maintenue pour observer le comportement à long terme. Les résultats montrent que le niveau de charge appliqué a affecté la distribution de la charge entre le radier et les pieux, et la répartition de la charge entre les pieux. Les pieux ont été efficaces pour supporter la charge et supprimer le tassement du RFP lorsque la charge appliquée était inférieure à la capacité ultime du groupe de pieux correspondant. Les résistances des fûts des pieux périphériques ont été mobilisées à partir des faibles niveaux de la charge appliquée tandis que la charge sur les pieux centraux était principalement supportée par les sections de pointe des pieux à ces niveaux de charge. Les résistances des fûts des pieux centraux ont été mobilisées aux niveaux supérieurs de la charge appliquée lorsque la charge appliquée dépassait la capacité ultime du groupe de pieux.

KEYWORDS: piled raft, clay ground, experiment, long-term settlement, pile load.

1 INTRODUCTION

The use of piled raft foundations (PRFs) in engineering constructions has become widespread in recent years because of their advantages, such as higher bearing capacity and smaller differential settlement. The behavior of PRFs has been investigated in many researches for several decades, in which a few researches investigated PRF behavior on clay ground subjected to vertical loads through physical modeling (e.g., Cooke 1986; Horikoshi and Randolph 1996; Dey and Ghosh 2016; Thoidingjam et al. 2016). In these researches, the behavior of PRFs was investigated for many aspects such as the effect of pile spacing, pile number, pile size and raft size on distributions of loads and settlements of PRFs until the end of the construction period when the full load was applied. However, from field measurement data, many cases have been reported of piled foundations on clay ground that the foundations begin to settle in construction period and continue to settle for a long period after the completion of the construction (ed. Hooper 1973; Sales et al. 2010; Tang et al. 2014). Furthermore, the load distribution of the foundation may also change for a long time after the construction work because of the changes of the stresses and strains in the ground, caused by ground consolidation. Therefore, when designing a PRF on clay, designers need to understand the behavior of PRF not only in the construction period but also in primary and secondary consolidation periods.

Hence, in this paper, the behavior of a PRF on saturated clay ground was investigated through small-scale physical modeling considering the effect of the consolidation processes. Focuses were placed on the pile response, on the foundation settlement, on the load sharing between the raft and the piles, and especially on the load sharing between the piles under different magnitudes of the applied loads. The changes of ground strength after the load test on PRF were also investigated to understand more about ground consolidation. Furthermore, the behaviors of individual piles and pile group were also investigated for comparison purposes.

2 EXPERIMENTAL DESCRIPTION

2.1 *Model ground*

The soil used for the model ground was a mixture of Kasaoka clay and Silica sand #6. Clay ground was prepared in a cylindrical chamber with a height of 420 mm and a diameter of 420 mm. A drainage line with a valve was connected to the bottom of the chamber, and with the valve either open or closed, the bottom surface of the model ground was either drained or undrained during consolidation process, respectively.

The model ground was prepared as follows: Firstly, Silica sand #3 was saturated and compacted in the chamber until it reached a high relative density D_r of about 81% and a thickness of 50 mm for a bottom drainage layer. This layer was considered as a stiff layer. Secondly, dry Kasaoka clay powder and Silica sand #6 were mixed at a mass ratio of 1:1 (K50S50) in a rectangular basin. Water was then added to the mixed soil to obtain a soil slurry with a water content of 1.3 *LL* (*LL*: liquid limit). This soil slurry was poured into the soil chamber to an initial thickness of 370 mm. The soil was left to consolidate under its self-weight for two days. After that, another Silica sand layer was placed on the clay to provide the top drainage layer, and a

rigid circular loading plate was placed on the top drainage layer. One load-cell was connected to the top center of the loading plate to measure the consolidation pressure and two dial gages were connected on the top surface of the loading plate at two symmetric locations to measure settlement of the ground surface during the consolidation stage. Next, vertical load on the loading plate was increased to consolidate the soil one-dimensionally in several steps up to vertical stress of 100 kPa. Each load step was maintained until the degree of consolidation reached 90% following Terzaghi's one-dimensional consolidation theory. The final load step was kept for one more week to have a higher degree of consolidation. Finally, the consolidation pressure was removed and the ground was allowed for the swelling process in 10 days. It is noticed that during the consolidation and swelling processes, the bottom drainage line was opened so that water could seep through both the top and bottom surfaces to reduce the consolidation time.

T-bar tests, cone penetration tests (CPTs), and unconfined compression tests (UCTs) were carried out immediately after completion of the load test on the model foundation to obtain properties of the model ground. The detailed descriptions of T-bar tests and CPTs were shown in Hoang and Matsumoto (2020a). Two T-bar tests (T1 and T2) and two CPTs (C1 and C2) were conducted at locations far from the load test area to obtain undrained shear strength c_u of the original model ground without the effect of loading test. Two T-bar tests (T3 and T4) and two CPTs (C3 and C4) were carried out at the locations beneath the raft base edge and one T-bar test (T5) was carried out at the location beneath the raft base center to catch how the load test of PRF affected the ground strength. c_u was deduced from the average stress acting on T-bar $q_{u\ T\text{-}bar}$ or cone tip resistance $q_{u\ cone\ tip}$ using the empirical equations proposed by Low et al. (2010):

$$c_u = q_{u\ T\text{-}bar}/ N_t \quad (1)$$

where N_T is the resistance factor for the T-bar and was taken as 10.5 after Low et al. (2010).

$$c_u = (q_{u\ cone\ tip} - \sigma_{vo})/ N_k \quad (2)$$

where σ_{vo} is the total overburden stress; N_k is the resistance factor for the cone tip was taken as 12 after Low et al. (2010).

As for UCTs, 5 soil specimens were recovered from the model ground at different depths from the ground surface. Soil specimens U1-U3 were sampled at the upper layer with an average depth of 100 mm from the raft base level, and soil specimens U4-U5 were sampled at the lower layer below the pile tip level with an average depth of 220 mm from the raft base level. The locations of specimens were also selected at (U4), near (U3), and far (U1, U2, and U5) from the loading area. c_u was estimated from unconfined compression strength q_u as $c_u = q_u /2$.

Figure 1(a) shows the locations of CPTs, T-bars, and UCTs.

Figure 1(b) shows the distributions of c_u with depth. In general, c_u varied with depth and c_u of the original model ground could be described approximately by the following equation:

$$c_u\ (\text{kPa}) = 9\ (\text{kPa}) + z\ (\text{mm}) \times 0.05\ (\text{kPa/mm}) \quad (3)$$

For the results of the distributions of c_u with depth under the loading area, the results were discussed later with the results of the load tests.

Other laboratory soil tests such as oedometer, Atterberg limits, density and water content of the soil were conducted to obtain other ground properties, and their results are summarized in Table 1.

2.2 *Model foundations*

Model piles used in this study were ABS (Acrylonitrile Butadiene Styrene) solid bars (Fig. 2(a)) having a diameter D of 10 mm and a length L of 150 mm. Young's modulus E_p and Poisson's ratio ν_p of the model piles are 2920 N/mm^2 and 0.406, respectively. In order to measure axial forces along each pile, strain gages were attached on the pile shaft at different levels as shown in Fig. 2(b). Model raft was a square aluminum plate with a thickness of 12 mm and a width B of 125 mm (Fig. 2(a)), and regarded as rigid.

In the experiment, the model foundation was a 16-pile pile foundation with a center-to-center pile spacing s equal to 3D. Figure 2(c) shows the dimensions of the foundation model.

Table 1. Properties of the model ground soil (called K50S50).

Parameter	Notation and unit	Value
Density of soil particle	ρ_s (Mg/m^3)	2.653
Saturated density	ρ_{sat} (Mg /m^3)	1.98
Plastic limit	PL (%)	13.6
Liquid limit	LL (%)	33.9
Plastic index	PI (%)	20.3
Compression index	C_c	0.291
Swelling index	C_s	0.055
Water content*	w (%)	26.2
Void ratio*	e	0.70

* after the consolidation with vertical pressure of 100 kPa

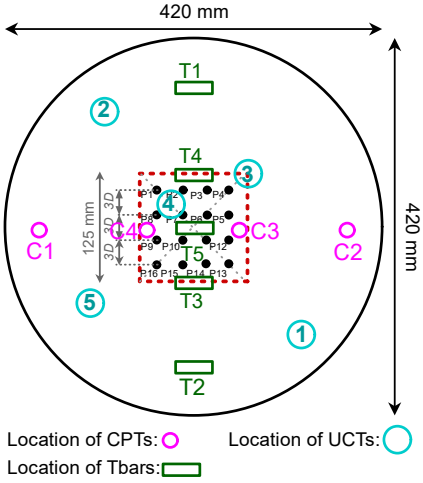

(a) locations of soil tests

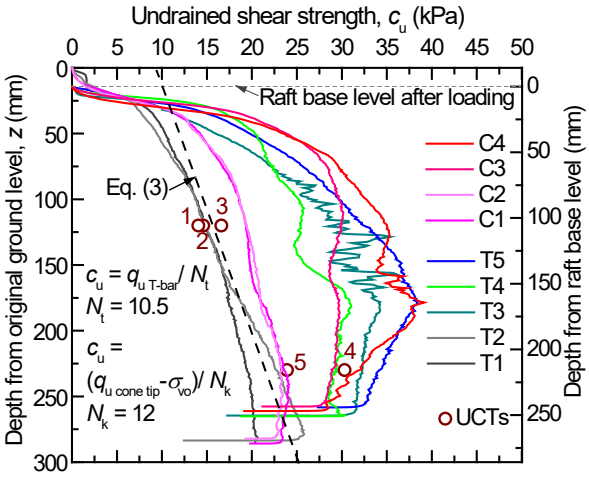

(b) Distributions of undrained shear strength with depth

Figure 1. Investigations of undrained shear strength.

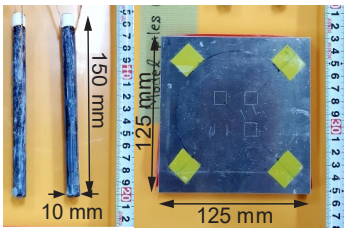

(a) Model piles and model raft

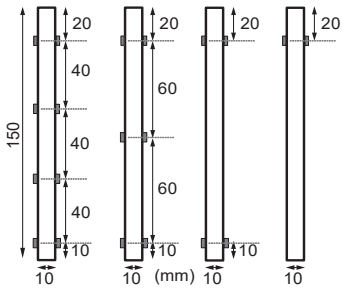

(b) Locations of strain gages

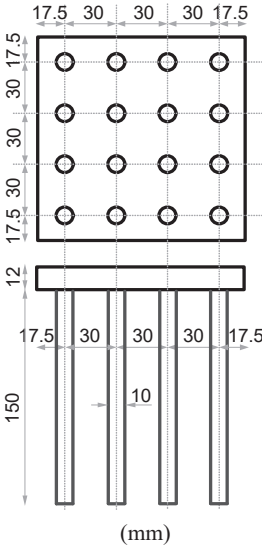

(c) Model foundation

Figure 2. Model piles, raft, and pile foundation.

2.3 *Instrumentations and test procedure*

Figure 3 shows the set-up of the experiment. The loading system included an air cylinder to apply constant vertical load, a load cell to measure the applied load and 4 dial gages to measure settlements of the foundation. One pore water pressure transducer and one earth pressure cell were installed at the locations near the raft base center.

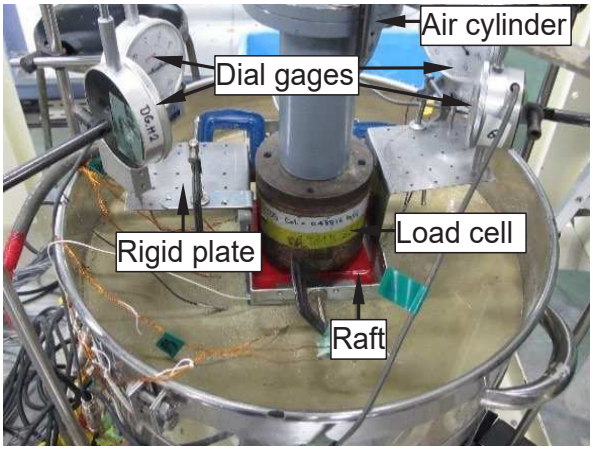

Figure 3. The set-up of experiments.

As for the load tests of the pile foundations, 16 piles were firstly jacked into the ground one by one with $s = 3D$ until the pile head had penetrated by 135 mm. One day after the completion of the pile installation, the vertical static load test (SLT) was conducted on each pile. Thereafter, the raft was placed on the pile heads with a gap between the raft base and the ground surface of around 7 mm, and SLT of the pile group (PG) was conducted in a displacement-controlled manner. The PG changed to piled raft (PR) after the raft base touched the ground surface. In the PR condition, vertical load was increased by multiple steps in a load-controlled manner and each load step was maintained for a sufficient time to obtain the long-term behavior of the foundation. Three first load steps were equal to 35%, 60%, and 95% of the ultimate capacity of PG, respectively. The next load steps were increased by 500 N for each step until the foundation settlement exceeded 10% of the raft width B (the settlement of 10% of B could be regarded as the ultimate condition after Cooke (1986)).

3 EXPERIMENTAL RESULTS

3.1 *Pile resistance during jacking installation process*

Figure 4 shows the pile resistance during the installation process of each pile and the order of pile installation was also shown on the figure. All the piles were jacked into the ground with the same constant displacement rate of 1 mm/s. Among 16 piles, P7 was jacked first, therefore P7 behaved as a single pile during the jacking process. The results show that 16 piles have almost equal resistances except for P2 and P15, which was equal to the pile resistance of the single pile (P7), therefore, the interaction among the piles in the jacking process was minor.

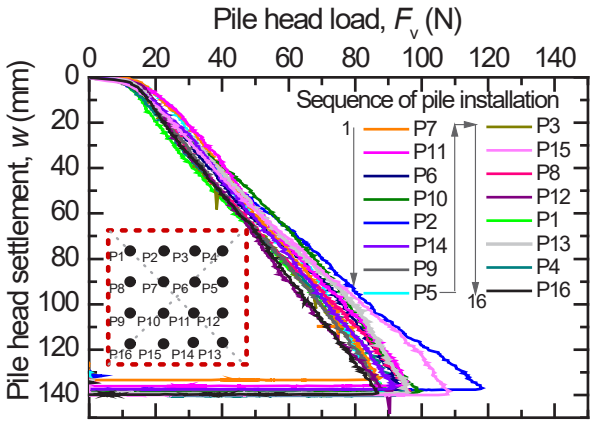

Figure 4. Load vs. settlement during jacking processes.

3.2 *Pile resistance during static load test of each pile*

Figure 5 shows the load-settlement curve of each pile during the SLT after the installation process of all the piles. The sequence of the SLT of each pile was also shown on the figure. Basically, the results show that the corner piles (P14, 4, 13, and 1), of which SLTs were conducted firstly, had higher resistances, in comparison with edge piles and center piles. Oppositely, the center piles (P10, 6, 11, and 7), of which SLTs were conducted lastly, had the lowest resistances. One of the possible reasons is that the SLT process of previous piles generated PWP and reduced lateral effective stresses of the surrounding soil. Consequently, the resistance of the piles, of which SLT were carried out later, became smaller.

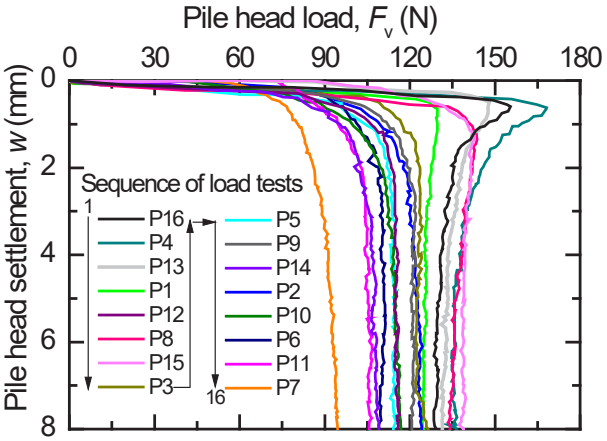

Figure 5. Load vs. settlement during static load test of each pile.

3.3 *Pile resistance during static load test of pile group*

Figure 6 shows the load-settlement curves during the SLT of the PG, including the load-settlement relationship of each pile (from SGs near the pile head), and the sum of 16 piles. Figure 6 shows

that the ultimate PG resistance was 2100 N and the average load carried by each pile was about 130 N, slightly higher than the average pile resistance of 120 N when the piles were subjected to SLT separately (Fig. 5). This indicates that the interaction among the piles when they were loaded at the same time increased the pile resistance. The measured results show that in PG condition, the average load carried by a corner pile was highest and that by a center pile was lowest among three types of pile position, this trend is similar to the pile behavior in SLT of each pile.

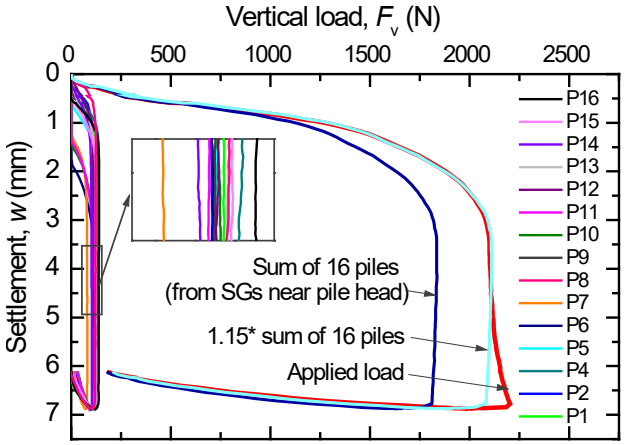

Figure 6. Load vs. settlement during SLT of pile group.

3.4 *Pile resistance during static load test of piled raft*

Figure 7 shows the changes of the applied load P, the settlement w, the load carried by the 16 piles P_p, and the load carried by the raft P_r for the whole PR experimental duration with 8 load steps.

Focusing first on the results of the first 3 load steps of P = 0.75 kN, 1.25 kN, and 2.0 kN, it is noted that the applied loads of the first 3 load steps were smaller than the ultimate capacity of the corresponding PG of about 2.1 kN (2100 N as shown in Figure 6). Figure 7 shows that the piles carried over 90% of the applied load in these load steps, and the foundation settlements of these load steps were also small. This indicates that when the applied load was small (smaller than the corresponding pile group ultimate capacity), the piles were effective at supporting the applied load and suppressing foundation settlement.

For the last 5 load steps, the increments of the settlement of the foundation were larger, and the changes of the settlement with time were more clearly, in comparison with the first 3 load steps. Figure 7 clearly shows that the foundation settlement occurred quickly when the applied load was increased, and it continued to increase for a long time after the completion of the increase of the applied load. The pile resistance firstly increased quickly with increasing applied load, and then pile resistance reduced a little bit. The reduction of pile resistance (softening behavior) when the applied load was increasing (load-increasing period) was already explained detailly by Hoang and Matsumoto (2020b). At early stages after the completion of the load-increasing period (primary consolidation stages), the pile resistance increased again with elapsed time. This phenomenon is due to the consolidation processes of the ground. As the pore water pressure which was generated during the load-increasing period dissipated with elapsed time, the corresponding effective ground stresses and the ground stiffness increased, which resulted in increase in pile resistance. The raft base resistance began to mobilize and increase gradually with increasing applied load. The raft supported less than 10% of the applied load at the first load step. At the final load step of P = 4.5 kN, the raft carried 27% (1.22 kN) of the total applied load. It is interesting that, although the raft shared only 27% of the PR ultimate capacity, the PR capacity was double of the PG ultimate capacity. This is because of the increment of pile resistance under the load transfer mechanism of piled raft condition. This phenomenon indicated the positive effect of PR condition on the pile resistance even for the saturated clay ground.

Let us consider how the pile resistance changes in PR condition. Figure 8 shows the increments of the average pile head loads with time of three types of pile position: corner pile, edge pile, and center pile. Among 3 pile positions, the pile head load of the center pile was basically the lowest in the first 3 load steps. The center pile head load then increased significantly during the last 5 load steps and became the highest in the final 4 load steps.

In contrast, the corner pile carried the highest load until the 4th load step (except for the 1st load step), thereafter, the increment of the corner pile head load became smaller than that of the center pile and the load carried by the corner pile became below that of the center pile at the final load step. The behavior of the edge pile was similar to that of the center pile at the first 4 load steps, but was similar to the behavior of the corner pile at the last 4 load steps. It is thought that this result was caused by the different increments of ground strength at the different pile locations as well as different load levels in the primary consolidation processes. This can be explained by the distributions of c_u after the load test, as shown in Fig. 1. This aspect will be discussed later again.

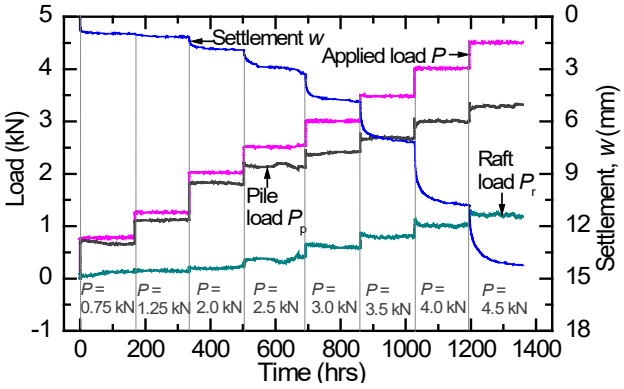

Figure 7. Load and settlement vs. time during SLT of PR.

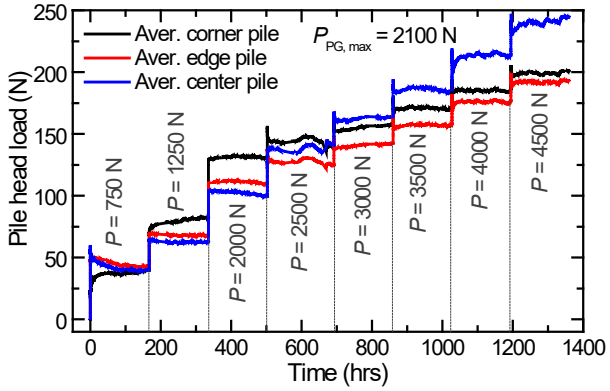

Figure 8. Changes of pile loads during long-term SLT of PR.

The increments of axial forces along a corner pile (P16, Fig. 9(a)), an edge pile (P15, Fig. 9(b)), and a center pile (P6, Fig. 9(c)) with normalized settlement w/D are shown in Fig. 9. The axial forces herein were obtained at the end of each load step.

Focusing first on the corner pile, for the first 3 load steps, the shaft resistance increased sharply meanwhile the tip resistance increased slightly. The shaft resistance supported up to 75% of the total pile load at the end of the 3rd load step. For the last 5 load steps, the tip resistance increased more considerably than the shaft resistance and finally supported about 1/3 of the pile load.

In contrast to the corner pile, the center pile had very small shaft resistance for the first 3 load steps, the pile load, therefore, was mainly carried by the bottom section of the pile. However,

the shaft resistance of the center pile increased significantly in the last 5 load steps and supported a noticeable part of the pile load at the final step (extrapolated as around 50%: the SGs at the pile tip of the center pile were damaged). Among the 3 piles, the load carried by the center pile was the largest at the final load step because of the large pile tip resistance, although the shaft resistance of the 3 piles was similar.

It is interesting that the tip resistance of the edge pile was almost equal to that of the corner pile. In the first 3 load steps, the shaft resistance of the edge pile was smaller than that of the corner pile but larger than that of the center pile. In the last 5 load steps, the increment of shaft resistance of the edge pile was slightly higher than that of the corner pile. The shaft resistance of the edge pile supported about 60% of the pile load at the final load step.

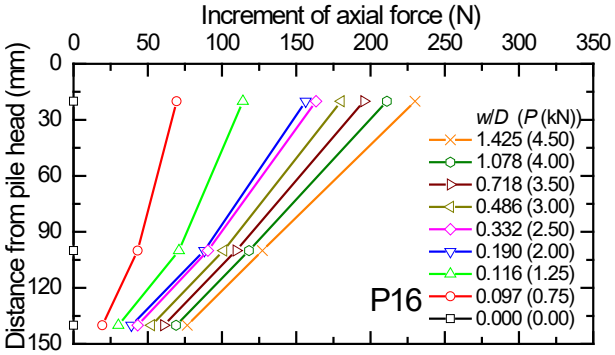

(a) Corner pile

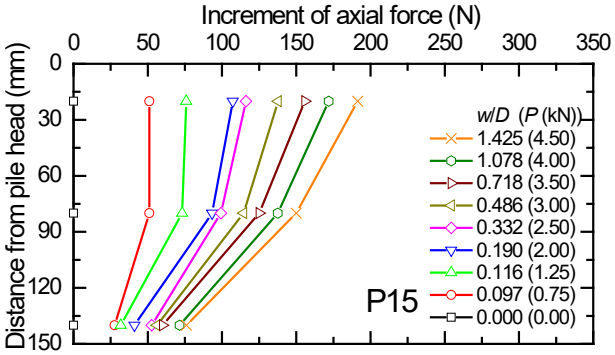

(b) Edge pile

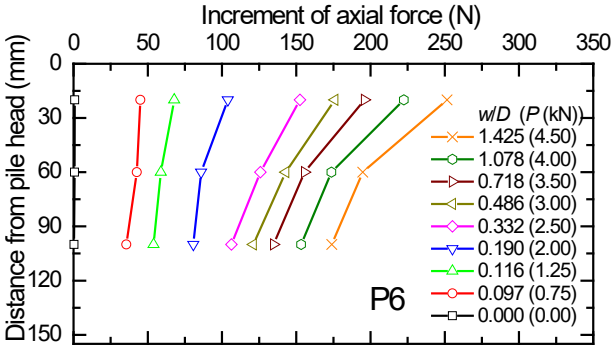

(c) Center pile

Figure 9. Changes of axial forces along piles during SLT of PR.

The increments of undrained shear strength c_u (estimated from T-bar tests, see Fig.1) beneath the raft base show a good agreement with the increments of the resistances of the 3 piles. After the load test, at the depth of 150 mm from the raft base (the pile tip level), the c_u at the center of the loading area (T5, area of the center piles) was larger than the c_u at the edge of the loading area (T3 and T4). The noticeable increases of the center pile load in the last 5 load steps indicate that the ground consolidation occurred significantly in the center area during these load steps.

Interestingly, the average load carried by each pile exceeded 200 N at the final load step, which was much larger than the ultimate capacity of each pile in the corresponding PG (average 130 N per pile). This result was also caused by the increase of ground strength in consolidation processes under PR condition.

4 CONCLUDING REMARKS

In this paper, pile behavior of a long-term vertically loaded piled raft model on saturated clay ground was investigated through small-scale physical modeling.

The experimental results showed that the level of applied load P affects the load sharing between the raft and the piles, and also affects the load sharing between piles. The piles were effective at supporting the applied load and suppressing PR settlement when the applied load on PR was smaller than the ultimate capacity of the corresponding PG $P_{PG,\ ultimate}$.

At small applied loads ($P < P_{PG,\ ultimate}$), average load carried by a corner pile was higher, compared to that of an edge pile and a center pile. However, at large applied loads, average load carried by a center pile was the highest among the three pile types.

The shaft resistances of peripheral piles were mobilized from the low level of applied load ($P < P_{PG,\ ultimate}$), but that of the center piles were mobilized at the higher level of applied load ($P > P_{PG,\ ultimate}$).

REFERENCES

Cooke R.W. 1986. Piled raft foundations on stiff clays—a contribution to design philosophy. *Géotechnique* 36(2), 169–203.

Dey R. and Ghosh A. 2016. Experimental investigation on behaviour of pile-raft foundation. *Indian Geotechnical Society, Kolkata Chapter, Geotechnics for Infrastructure Development*, 11th – 12th March 2016, Kolkata, West Bengal, India.

Horikoshi K. and Randolph M.F. 1996. Centrifuge modelling of piled raft foundations on clay. *Géotechnique* 46(4), 741–752.

Hoang L. and Matsumoto T. 2020a. Time-dependent behaviour of piled raft foundations on saturated clay: experimental investigations. *Int. J. of GEOMATE* 18(66), 1–8.

Hoang L.T. and Matsumoto T. 2020b. Long-term behavior of piled raft foundation models supported by jacked-in piles on saturated clay. *Soils and Foundations* 60(1), pp. 198–217.

Hooper J.A. 1973. Observations on the behaviour of a piled-raft foundation on London clay. *Proceedings of the Institution of Civil Engineers* 55(4), 855–877.

Low H.E., Lunne T., Andersen K.H., Sjursen M.A., Li X. and Randolph M.F. 2010. Estimation of intact and remoulded undrained shear strengths from penetration tests in soft clays. *Géotechnique* 60(11), 843–859.

Sales M.M., Small J.C. and Poulos H.G. 2010. Compensated piled rafts in clayey soils: Behaviour, measurements, and predictions. *Can. Geotech. J.* 47(3), 327–345.

Tang Y.J., Pei J. and Zhao X.H. 2014. Design and measurement of piled-raft foundations. *Proc. Inst. Civ. Eng. Geotech. Eng.* 167(5), 461–475.

Thoidingjam D., Prasad D.S.V. and Devi K.R. 2016. Effect of number of pile in pile-raft system in organic clay. *IOSR Journal of Mechanical and Civil Engineering* 13(4), 83–88.